Robust A Posteriori Error Estimation for Non-Conforming Finite Element Approximation

Mark Ainsworth*

25th March 2003

Abstract

The equilibrated residual method for a posteriori error estimation is extended to non-conforming finite element schemes for the approximation of Darcy's equation governing flow in porous media, where the permeability is allowed to undergo large jumps in value across interfaces between differing media. The estimator is shown to provide a computable upper bound on the error, and, up to a constant independent of the mesh-size, provides two-sided bounds on the error. The robustness of the estimator is also studied and the dependence of the constant on jumps in permeability is given explicitly.

Key words. Robust a posteriori error estimation. Non-conforming finite element. Crouzeix–Raviart element. Saturation assumption. Darcy's equation.

AMS subject classifications. Primary 65N30. Secondary 65N15, 65N50, 76S05.

1 Introduction

A posteriori error estimation for *conforming* finite element schemes has been the subject of extensive investigation and such methods are now routinely incorporated in adaptive finite element procedures by the engineering and scientific computing community. In contrast, the treatment of *non-conforming* methods [8] has been subject to sporadic yet sustained attention over the past decade.

The early work of Agouzal [1] was concerned with a posteriori error estimation for non-conforming finite element approximation of Poisson type problems. The important contribution of Dari *et al.* [10] presented an explicit a posteriori error estimator based on evaluation of norms of residuals supplemented by jumps in fluxes across inter-element edges, and showed that the

*Mathematics Department, Strathclyde University, 26 Richmond Street, Glasgow G1 1XH, Scotland. M.Ainsworth@strath.ac.uk. Support for this work from the Leverhulme Trust through a Leverhulme Trust Fellowship is gratefully acknowledged. This work was completed while the author was visiting the Newton Institute for Mathematical Sciences, Cambridge, UK. It is a pleasure to thank Prof. Dr. Willy Dörfler for his comments on an earlier version of the manuscript.

estimator provides two-sided bounds on the error up to generic, unknown constants that are independent of the mesh size. This was subsequently extended to non-conforming mixed finite element approximation of Stokes flow [9] and non-Newtonian flow [3]. The application of hierarchic basis estimators to non-conforming finite element approximation was considered by Hoppe and Wohlmuth [15], where the usual hierarchic basis estimator is augmented with an additional term comparing the non-conforming approximation with a smoothed approximation. Two-sided bounds were obtained [15] under the assumption that a saturation condition is valid. In a related approach, Schieweck [17] proposed a residual based estimator supplemented with the same additional term as in [15]. However, the analysis of efficiency in [17] was based on additional rather strong assumptions on the regularity of the mesh and the true solution. Carstensen *et al.* [6], derived estimators based on *gradient* averaging (or smoothing) techniques and obtained two-sided bounds. All of the above estimators involve generic, unknown constants, and as such provide refinement indicators rather than actual numerical bounds on the error.

Destuynder and Métivet [12] derived a posteriori bounds for the error in a conforming approximation obtained by smoothing the non-conforming approximation. Explicit, computable upper bounds on the error measured in the energy norm were obtained for approximation of Poisson's equation. In order to show the bounds are efficient, the authors made additional regularity assumptions on the mesh and the true solution, and showed that the estimator decays at the same rate as the true error. Unfortunately, these regularity assumptions on the mesh and the true solution generally fail to hold in the context of the solution of practical problems on adaptively refined meshes.

A technique that has proved particularly effective and robust for a posteriori estimation of the error in *conforming* finite element schemes is the *equilibrated residual method*, as described for example in [2]. One goal of the present work is to extend the equilibrated residual method to non-conforming finite element schemes for the approximation of Darcy's equation governing flow in porous media. The permeability is assumed to be piecewise constant on subdomains corresponding to different media, but is allowed to undergo large jumps across interfaces. Particular attention is paid to the robustness of the a posteriori error estimator with respect to the size of the jumps. This issue has also been studied in the setting of conforming finite element approximation by Bernardi and Verfürth [4].

The approach is based on the idea of Dari *et al.* [10] involving an orthogonal (Helmholtz) decomposition of the error into a conforming part and a non-conforming part. The conforming part is treated using a modification of the standard equilibrated residual method where the weakened continuity requirements for a non-conforming element are fully exploited. Indeed, the usual procedure for conforming approximation can be dramatically simplified to the extent that in its final form the estimator resembles an explicit estimator with, however, the advantage that there are no unknown constants. The remaining non-conforming part of the error is estimated using the difference between the non-conforming approximation and a smoothed non-conforming approximation similarly to [15], and this is shown to give an upper bound without recourse

to unknown constants. The final form of the estimator resembles those derived in [10, 12, 15, 17]. However, one by-product of the method of derivation is that the estimator can be shown to provide computable upper bounds on the error– a feature characteristic of the equilibrated residual method. Furthermore, the bounds are shown to be efficient in the sense that the estimator is bounded above by the true error up to a constant independent of any mesh-size. This result is proved without additional assumptions on the regularity of the true solution and the mesh is allowed to be locally refined, as would be the case of adaptive refinements. However, in order to circumvent the saturation assumption [15], we shall assume that the oscillation of the data is sufficiently small. This extends the ideas of Dörfler and Nochetto [13] to non-conforming finite element approximation. Moreover, the analysis takes full account of the large jumps in the permeability across material interfaces, and shows that the estimator is robust with respect to the jumps in certain circumstances (such as if the hypothesis assumed by Bernardi and Verfürth [4] is satisfied).

Gradient smoothing procedures are frequently adopted in the setting of conforming finite element approximation. However, for the non-conforming schemes considered here, smoothing is applied directly to the (discontinuous) finite element approximation, as opposed to its gradient. Interestingly, in the case of Laplace's equation, the exact solution of the local residual problem vanishes identically. This means that the estimator reduces to a recovery based estimator, and in view of the upper bound property, we arrive at the somewhat surprising conclusion that the recovery based estimator provides a guaranteed upper bound on the error (even though the true solution may have singularities and the mesh may be highly unstructured).

The remainder of this paper is organised as follows. After describing the details of the finite element scheme and the conditions on the mesh, the decomposition of the error into a conforming and non-conforming component is presented. The main results of the paper are then outlined, and illustrative numerical examples are presented. Subsequent sections are concerned with the derivation of the upper and lower bounds for each source of error.

2 Preliminaries

2.1 Model Problem

Consider Darcy's equation governing flow through a porous medium

$$-\mathbf{div}(A\,\mathbf{grad}\,u) = f \text{ in } \Omega \tag{1}$$

subject to $u = q$ on Γ_D and $\boldsymbol{n}\cdot A\,\mathbf{grad}\,u = g$ on Γ_N, where Ω is a plane polygonal domain, the disjoint sets Γ_D and Γ_N form a partitioning of the boundary $\Gamma = \partial\Omega$ of the domain. The data satisfy $f \in L_2(\Omega)$, $g \in L_2(\Gamma_N)$, $q \in H^1(\Gamma_D)$ and $A \in L_\infty(\Omega; \mathbb{R}^{2\times 2})$ is positive definite. For simplicity, it will be assumed that the permeability matrix A is piecewise constant on sub-domains of Ω. However, the value of A across a sub-domain boundary may undergo jumps of many orders of magnitude, corresponding to transition between regions of widely differing permeability.

The variational form of the problem consists of finding $u \in H^1(\Omega)$ such that $u = q$ on Γ_D and

$$(A\,\mathbf{grad}\,u, \mathbf{grad}\,v) = (f, v) + \int_{\Gamma_N} gv\,\mathrm{d}s \quad \forall v \in H^1_E(\Omega) \tag{2}$$

where $H^1_E(\Omega) = \{v \in H^1(\Omega) : v = 0 \text{ on } \Gamma_D\}$. In general, we shall use the notation $(\cdot,\cdot)_\omega$ to denote the integral inner product over a region ω, and omit the subscript in the case where ω is the physical domain Ω.

Consider a family of partitions $\{\mathcal{P}\}$ of the domain Ω into the union of non-overlapping, shape regular triangular elements such that the non-empty intersection of a distinct pair of elements is a single common node or single common edge. The family of partitions is assumed to be locally quasi-uniform in the sense that the ratio of the diameters of any pair of neighbouring elements is uniformly bounded above and below over the whole family.

In addition, whenever possible, the partitioning is chosen to reflect the structure of the permeability matrix in the sense that individual elements do not straddle a sub-domain boundary where the value of A undergoes a large jump. This requirement is reflected in the assumption that, for every element $K \in \mathcal{P}$, there exist positive constants λ_K and Λ_K satisfying

$$\lambda_K \|\boldsymbol{p}\|^2_{L_2(K)} \le (A\boldsymbol{p}, \boldsymbol{p})_K \le \Lambda_K \|\boldsymbol{p}\|^2_{L_2(K)} \quad \boldsymbol{p} \in L_2(K)^2 \tag{3}$$

such that the ratio $\Upsilon_K = \Lambda_K/\lambda_K$ is uniformly bounded over the whole family of partitions. It will be important to develop a posteriori error estimators whose reliability and efficiency is insensitive to the magnitude of the jumps in permeability between differing regions, but which are allowed to depend on the variation of A within a region.

2.2 Non-conforming Finite Element Approximation

Let $\mathcal{N}$ index the set of element vertices, $\partial\mathcal{P}$ denote the set of element edges, $\mathcal{M} = \{\boldsymbol{m}_\gamma : \gamma \in \partial\mathcal{P}\}$ denote the set of points located at midpoints of edges and let $\mathbb{P}_1$ denote the space of polynomials of total degree at most one. The *Crouzeix–Raviart* finite element space [8] is defined by

$$X^{\mathsf{nc}} = \left\{v : \Omega \to \mathbb{R} : v_{|K} \in \mathbb{P}_1 \quad \forall K \in \mathcal{P}, \quad v \text{ is continuous at } \boldsymbol{m}_\gamma \in \mathcal{M}\backslash\Gamma\right\}$$

with the subspace X^{nc}_E defined by

$$X^{\mathsf{nc}}_E = \{v \in X^{\mathsf{nc}} : v(\boldsymbol{m}_\gamma) = 0 \text{ for } \gamma \subset \Gamma_D\}\,.$$

Functions belonging to the space X^{nc} and X^{nc}_E may have discontinuities across element interfaces, meaning that X^{nc} is not a subspace of $H^1(\Omega)$ and therefore constitutes a *non-conforming* approximation space [5, 7]. The non-conforming finite element approximation of problem (2) consists of finding $u_{\mathsf{nc}} \in X^{\mathsf{nc}}$ such that

$$\begin{aligned} (A\,\mathbf{grad}_{\mathsf{nc}}\,u_{\mathsf{nc}}, \mathbf{grad}_{\mathsf{nc}}\,v) &= (f, v) + \textstyle\int_{\Gamma_N} gv\,\mathrm{d}s \quad \forall v \in X^{\mathsf{nc}}_E \\ u_{\mathsf{nc}}(\boldsymbol{m}_\gamma) &= q(\boldsymbol{m}_\gamma) \quad \forall \gamma \subset \Gamma_D \end{aligned} \tag{4}$$

where $\mathbf{grad}_{\mathsf{nc}}$ denotes the operator defined by

$$(\mathbf{grad}_{\mathsf{nc}}\, v)_{|K} = \mathbf{grad}(v_{|K}), \quad K \in \mathcal{P}.$$

A Lagrange type basis $\{\theta_\gamma\}$ for the space X^{nc} may be constructed by choosing $\theta_\gamma \in X^{\mathsf{nc}}$ to be the function uniquely defined by the conditions

$$\theta_\gamma(\boldsymbol{m}_{\gamma'}) = \delta_{\gamma\gamma'}, \quad \gamma' \in \partial\mathcal{P}. \tag{5}$$

A non-conforming interpolation operator $\Pi_{\mathsf{nc}} : H^1(\Omega) \to X^{\mathsf{nc}}$ is defined by the conditions

$$\int_\gamma \Pi_{\mathsf{nc}}\, v \,\mathrm{d}s = \int_\gamma v \,\mathrm{d}s \quad \forall \gamma \in \partial\mathcal{P}. \tag{6}$$

The representation of the operator relative to the basis (5) is given by

$$\Pi_{\mathsf{nc}}\, v = \sum_{\gamma\subset\partial\mathcal{P}} \overline{v}_\gamma \theta_\gamma \tag{7}$$

where $\overline{v}_\gamma$ denotes the average value of v on an edge γ. Observe that the restriction of $\Pi_{\mathsf{nc}}\, v$ to a particular element K is defined entirely in terms of the averages of the function v on the edges of the element and, moreover, Π_{nc} locally preserves constants. These properties (in conjunction with standard scaling arguments) may be used to deduce that there exists a positive constant C independent of any mesh-size such that the following local element-wise approximation property holds:

$$\|v - \Pi_{\mathsf{nc}}\, v\|_{L_2(K)} + h_K^{1/2} \|v - \Pi_{\mathsf{nc}}\, v\|_{L_2(\partial K)} \leq C h_K \|\mathbf{grad}\, v\|_{L_2(K)}\,. \tag{8}$$

2.3 Data Oscillation

It will be necessary to impose some notion of regularity of the underlying problem. Often, a *saturation condition* [15] is assumed, but this assumption makes reference to the (unknown) true solution u meaning that it is difficult to verify a priori. Dörfler and Nochetto [13], working in the context of conforming piecewise affine approximation, showed that the saturation assumption can be removed in favour of an assumption on the magnitude of the *data oscillation*. This condition has the advantage of being formulated directly in terms of the known data for the problem and can therefore be verified a priori. We shall show that a similar conclusion holds in the non-conforming setting considered here.

The oscillation of the data $f \in L_2(\Omega)$ over the finite element partition $\mathcal{P} = \{K\}$ is defined by

$$\mathrm{osc}(f, \{K : K \in \mathcal{P}\})^2 = \sum_{K\in\mathcal{P}} \mathrm{meas}(K) \left\|f - \overline{f}_K\right\|^2_{L_2(K)}. \tag{9}$$

where $\overline{f}_K$ is the average value of f over element K. The data oscillation quantifies the variation in the data f with respect to the partition $\mathcal{P}$. Likewise, the oscillation of the Neumann data g is defined by

$$\mathrm{osc}(g, \{\gamma : \gamma \subset \Gamma_N\})^2 = \sum_{\gamma\subset\Gamma_N} \mathrm{meas}(\gamma) \left\|g - \overline{g}_\gamma\right\|^2_{L_2(\gamma)}.$$

The appropriate quantity for the Dirichlet data turns out to be

$$\operatorname{osc}\left(\partial q/\partial s, \{\gamma : \gamma \subset \Gamma_D\}\right)^2 = \sum_{\gamma \subset \Gamma_D} \operatorname{meas}(\gamma) \left\| \frac{\partial q}{\partial s} - \mu_\gamma \right\|^2_{L_2(\gamma)} .$$

Here $\overline{g}_\gamma$ and μ_γ denote the average value of g and $\partial q/\partial s$ on edge γ.

2.4 Path Permeability

Let Ω_n denote the patch composed from those elements with a vertex located at $\boldsymbol{x}_n$, and let K, $K' \subset \Omega_n$ be distinct elements. It is useful to introduce the notion of permeability $\lambda_{KK'}$ between a pair of elements. Roughly speaking, this measures the permeability of the 'most permeable' route between the elements. The precise definition is based on the observation that there is always at least one connected path $\wp(K, K')$ passing from K to K' through adjacent elements belonging to the patch Ω_n. The smallest permeability of all the elements in the path $\wp(K, K')$ is given by $\min\{\lambda_M : M \in \wp(K, K')\}$. If $\boldsymbol{x}_n$ is an interior vertex, then there are two such paths and in this case we take $\wp(K, K')$ to be the path $\wp^*(K, K')$ which maximises the value of this quantity, and define

$$\lambda_{KK'} = \min\left\{\lambda_M : M \in \wp^*(K, K')\right\}. \tag{10}$$

If a vertex $\boldsymbol{x}_n$ of element K lies on the Dirichlet boundary Γ_D, then the element may be linked to Γ_D by a connected path $\wp(K, \Gamma_D)$ passing through adjacent elements as before. The permeability $\lambda_{K\Gamma_D}$ between element K and the Dirichlet boundary is then defined using (10) with $\wp^*(K, \Gamma_D)$ in place of $\wp^*(K, K')$. The ratio

$$\Upsilon_{KK'} = \frac{\min(\Lambda_K, \Lambda_{K'})}{\lambda_{KK'}} \tag{11}$$

measures path permeability relative to the least permeable of the two elements K and K' at the endpoints of the path.

If Ω_n is contained either within a sub-domain, on the interface between two sub-domains or at the cross-point of three sub-domains, then the relative path permeability is always unity, see Fig. 1(a)-(b). However, the relative path permeability may be arbitrarily large at cross-points where four or more sub-domains meet, as would be the case in Fig. 1(c) if $\alpha \ll 1$. This means that the relative path permeability remains bounded only under additional hypotheses. For example, if, as in Bernardi and Verfürth [4, Hypothesis 2.7], it is assumed that there is always a path between any two elements on which the permeability increases monotonically, then the relative path permeability is always unity, even at boundary nodes $\boldsymbol{x}_n \in \Gamma_D$.

3 A Posteriori Error Estimator

3.1 Decomposition of the Error

The purpose of the present work is to develop methods for obtaining computable estimators for the error $e = u - u_{\mathsf{nc}}$ in the non-conforming approximation mea-

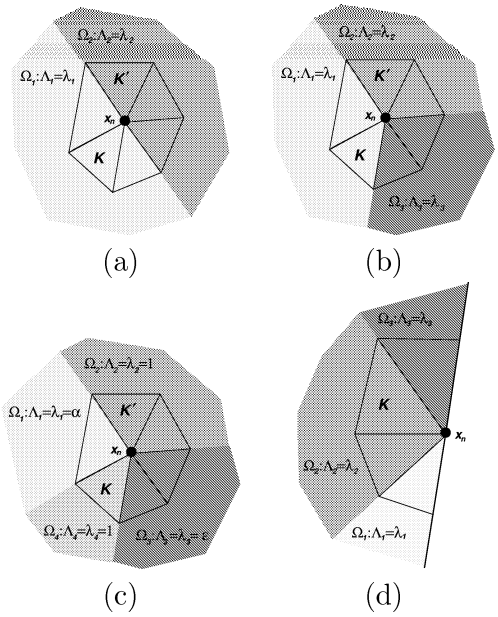

Figure 1: Value of relative path permeability (11) for some typical configurations. (a) Node on interface: $\Upsilon_{KK'} = 1$. (b) Node at cross-point of three sub-domains. $\Upsilon_{KK'} = 1$. (c) Node at cross-point of four sub-domains ($\epsilon \ll 1$). $\Upsilon_{KK'} = 1/\max(\min(1,\alpha),\epsilon)$. (d) Node on Dirichlet boundary. $\Upsilon_{K\Gamma_D} = \Lambda_2/\max(\min(\lambda_1,\lambda_2),\min(\lambda_2,\lambda_3))$.

sured in the energy norm denoted by $(A\,\mathbf{grad}_{\mathsf{nc}}\, e, \mathbf{grad}_{\mathsf{nc}}\, e)^{1/2}$. The following Helmholtz type decomposition is essentially taken from Dari *et al.* [10].

Lemma 1 *Let*

$$\mathcal{H} = \left\{ w \in H^1(\Omega) : \int_\Omega w \,\mathrm{d}\boldsymbol{x} = 0 \text{ and } \frac{\partial w}{\partial s} = 0 \text{ on } \Gamma_N \right\}.$$

The error e may be decomposed in the form

$$A\,\mathbf{grad}_{\mathsf{nc}}\, e = A\,\mathbf{grad}\,\phi + \mathbf{curl}\;\psi \tag{12}$$

where $\phi \in H^1_E(\Omega)$ satisfies

$$(A\,\mathbf{grad}\,\phi, \mathbf{grad}\, v) = (A\,\mathbf{grad}_{\mathsf{nc}}\, e, \mathbf{grad}\, v) \quad \forall v \in H^1_E(\Omega) \tag{13}$$

and $\psi \in \mathcal{H}$ satisfies

$$(A^{-1}\,\mathbf{curl}\;\psi, \mathbf{curl}\, w) = (\mathbf{grad}_{\mathsf{nc}}\, e, \mathbf{curl}\, w) \quad \forall w \in \mathcal{H}. \tag{14}$$

Moreover,

$$(A\,\mathbf{grad}_{\mathsf{nc}}\, e, \mathbf{grad}_{\mathsf{nc}}\, e) = (A\,\mathbf{grad}\,\phi, \mathbf{grad}\,\phi) + (A^{-1}\,\mathbf{curl}\;\psi, \mathbf{curl}\;\psi). \tag{15}$$

Proof. An application of the Lax-Milgram lemma shows that ϕ exists and is unique. Denote $\boldsymbol{w} = A(\mathbf{grad}_{\mathsf{nc}}\, e - \mathbf{grad}\,\phi) \in L_2(\Omega)^2$. With the aid of Green's formula and equation (13), we deduce that

$$0 = \int_\Omega v\,\mathbf{div}\boldsymbol{w}\,\mathrm{d}\boldsymbol{x} + \int_\Gamma v\,\boldsymbol{n}\cdot\boldsymbol{w}\,\mathrm{d}s \quad \forall v \in H^1_E(\Omega).$$

Consequently, $\boldsymbol{w}$ is divergence free in Ω and $\boldsymbol{n}\cdot\boldsymbol{w} = 0$ on Γ_N. Applying Theorem 3.1 in [14] shows that there exists $\psi \in H^1(\Omega)/\mathbb{R}$ such that

$$A(\mathbf{grad}_{\mathsf{nc}}\, e - \mathbf{grad}\,\phi) = \boldsymbol{w} = \mathbf{curl}\,\psi.$$

Furthermore, $\boldsymbol{n}\cdot\mathbf{curl}\,\psi = \boldsymbol{n}\cdot\boldsymbol{w} = 0$ on Γ_N, and we conclude that $\psi \in \mathcal{H}$. The characterisation (14) and the orthogonality property (15) hold provided that

$$\int_\Omega \mathbf{grad}\,\phi\cdot\mathbf{curl}\,w\,\mathrm{d}\boldsymbol{x} = 0 \quad \forall w \in \mathcal{H}.$$

This follows directly from an integration by parts on recalling that ϕ vanishes on Γ_D while $\boldsymbol{n}\cdot\mathbf{curl}\,w$ vanishes on Γ_N. □

Lemma 1 means that the error e in the non-conforming approximation may be split into two parts, as in equation (12). The nature of the contributions ψ and ϕ defined in Lemma 1 may be identified as follows. First, suppose that the non-conforming approximation u_{nc} happens to be conforming, by which we mean $u - u_{\mathsf{nc}} \in H^1_E(\Omega)$. The right hand side of equation (14) then simplifies to

$$(\mathbf{grad}_{\mathsf{nc}}\, e, \mathbf{curl}\,w) = (\mathbf{grad}\, e, \mathbf{curl}\,w) = \int_\Gamma e\,\boldsymbol{n}\cdot\mathbf{curl}\,w\,\mathrm{d}s = 0,$$

since e vanishes on Γ_D and $\boldsymbol{n}\cdot\mathbf{curl}\,w = 0$ on Γ_N for $w \in \mathcal{H}$. Hence, if the approximation u_{nc} is conforming, then the contribution ψ vanishes. For this reason, we shall refer to ψ as the *non-conforming error*. The remaining contribution, ϕ is referred to as the *conforming error*.

The splitting of the error into non-conforming and conforming components defines an orthogonal decomposition in the sense that the Pythagorean identity (15) holds. This means that the problem of obtaining a posteriori error estimators for the total error reduces to the derivation of estimators for the conforming and non-conforming errors *independently*. An estimator for the total error is then given by summing the estimators for the independent contributions.

3.2 Overview of Main Results

For ease of exposition, we state the main results proved in Sect. 5 and 6 assuming the data oscillation vanishes. For $K \in \mathcal{P}$, let $\boldsymbol{\sigma}_K$ denote the function $\boldsymbol{\sigma}_K = -\frac{1}{2}\overline{f}_K(\boldsymbol{x} - \boldsymbol{x}_K)$, where $\boldsymbol{x}_K$ denotes the element centroid, then direct evaluation reveals that

$$\eta^2_{\mathsf{cf},K} = \left(A^{-1}\boldsymbol{\sigma}_K, \boldsymbol{\sigma}_K\right)_K = \frac{1}{48}\,\mathrm{meas}(K)\overline{f}^2_K \sum_{\ell=1}^{3} \boldsymbol{w}_\ell^\top A^{-1}\boldsymbol{w}_\ell \tag{16}$$

where $\boldsymbol{w}_\ell$ is the position vector of vertex ℓ of the element relative to the centroid. This quantity defines an upper bound for the conforming error, as shown by combining Lemma 2 and Theorem 6 to obtain:

$$(A\,\mathbf{grad}\,\phi, \mathbf{grad}\,\phi) \leq \sum_{K\in\mathcal{P}} \eta_{\mathsf{cf},K}^2.$$

Moreover, Theorem 6 implies that this bound is efficient in the sense that

$$\eta_{\mathsf{cf},K}^2 \leq C\Upsilon_K(A\,\mathbf{grad}\,\phi, \mathbf{grad}\,\phi)_K$$

for all $K \in \mathcal{P}$. The estimator for the non-conforming error is defined in terms of a piecewise affine function $S(u_{\mathsf{nc}})$ on $\mathcal{P}$ obtained by smoothing the non-conforming approximation with values at vertices given by

$$S(u_{\mathsf{nc}})(\boldsymbol{x}_n) = \begin{cases} q(\boldsymbol{x}_n), & \text{if } \boldsymbol{x} \in \Gamma_D \\ \displaystyle\sum_{K\in\Omega_n} \omega_{K,n}\, u_{\mathsf{nc}|K}(\boldsymbol{x}_n), & \text{otherwise} \end{cases} \tag{17}$$

where the weights $\omega_{K,n}$ are defined by

$$\omega_{K,n} = \frac{\Lambda_K^{1/2}}{\sum_{K'\subset\Omega_n} \Lambda_{K'}^{1/2}}. \tag{18}$$

Any choice of weights satisfying the condition

$$\sum_{K\subset\Omega_n} \omega_{K,n} = 1. \tag{19}$$

is permissible. The requirement (19) leaves considerable latitude in the selection of the weights. For instance, one might even choose all but one of weights to vanish as suggested by Schieweck [17]. The obvious choice whereby the weights are chosen to be equal has been utilised by Oswald [16] in the context of multi-grid methods. An alternative choice, advocated by Destuynder and Métivet [12, eq. (17)], is to take $\omega_{K,n}$ proportional to the area of element K. If the mesh is locally quasi-uniform, then the latter two choices are not significantly different. Here, we are specifically concerned with the approximation of problems with highly varying local permeability, and the choice of weights given in (18) reflects this by depending on the value of the local permeability. The weights (18) are equal if the node $\boldsymbol{x}_n$ is located inside a sub-domain where the local permeability is constant, but differ markedly on interfaces and cross-points between sub-domains.

The estimator for the non-conforming error on element K is given by

$$\eta_{\mathsf{nc},K}^2 = (A\,\mathbf{grad}_{\mathsf{nc}}(u_{\mathsf{nc}} - S(u_{\mathsf{nc}})), \mathbf{grad}_{\mathsf{nc}}(u_{\mathsf{nc}} - S(u_{\mathsf{nc}})))_K\,. \tag{20}$$

Lemma 8 shows that the non-conforming error is bounded above by

$$\left(A^{-1}\,\mathbf{curl}\;\psi, \mathbf{curl}\;\psi\right) \leq \sum_{K\in\mathcal{P}} \eta_{\mathsf{nc},K}^2,$$

Ndofs	True	Estimated	Effectivity
44	8.87(-2)	2.26(-1)	1.60
99	4.02(-2)	9.97(-2)	1.57
154	2.15(-2)	5.15(-2)	1.55
209	1.41(-2)	3.25(-2)	1.52
264	1.11(-2)	2.50(-2)	1.50
446	5.86(-3)	1.35(-2)	1.52
640	3.86(-3)	8.84(-3)	1.51
933	2.60(-3)	5.96(-3)	1.51
1487	1.57(-3)	3.57(-3)	1.51

Table 1: Comparison of estimated and true error for L-shaped domain.

while Theorem 10 shows this bound is efficient in the sense that

$$\eta_{\mathsf{nc},K}^2 \leq C\Upsilon_{KK'} \left(A^{-1}\,\mathbf{curl}\;\psi, \mathbf{curl}\;\psi\right)_{\widetilde{K}}.$$

where $\widetilde{K}$ is the patch composed from element K along with its neighbours.

The above results show that the total error is bounded above by the sum of the local estimator (16) for the conforming error and the non-conforming error (20)

$$(A\,\mathbf{grad}_{\mathsf{nc}}\,e, \mathbf{grad}_{\mathsf{nc}}\,e) \leq \sum_{K\in\mathcal{P}} \left(\eta_{\mathsf{cf},K}^2 + \eta_{\mathsf{nc},K}^2\right). \tag{21}$$

This estimator is reminiscent of the estimators found in [10, 12, 15, 17]. Here, it is shown that the estimator provides a numerical upper bound for the total global error which does not involve unknown constants. Moreover, the estimator (21) is shown to be efficient and robust, without additional assumptions on the regularity of the true solution or on the mesh.

4 Numerical Examples

The behaviour of the estimator (21) is illustrated for some simple representative problems in this section.

4.1 Laplacian on L-shaped domain

Figure 2 shows the sequence of adaptively refined meshes for the solution of Laplace's equation on an L-shaped domain with pure Dirichlet boundary conditions chosen so that the solution is given by $u(r,\theta) = r^{2/3}\sin(2\theta/3)$. The conforming error vanishes in this case and the local error estimator on element K reduces to $\eta_{\mathsf{nc},K}$. The effectivity index is found to vary in the range 1.5-1.6 in this example, as shown in Table 1. The sequence of meshes was constructed adaptively by selecting for refinement all elements where the local error indicator exceeds 30% of the value of the largest local indicator.

4.2 Non-zero source term

Figure 3 shows the sequence of adaptively refined meshes for the solution of Poisson's equation with homogeneous Dirichlet boundary conditions and source

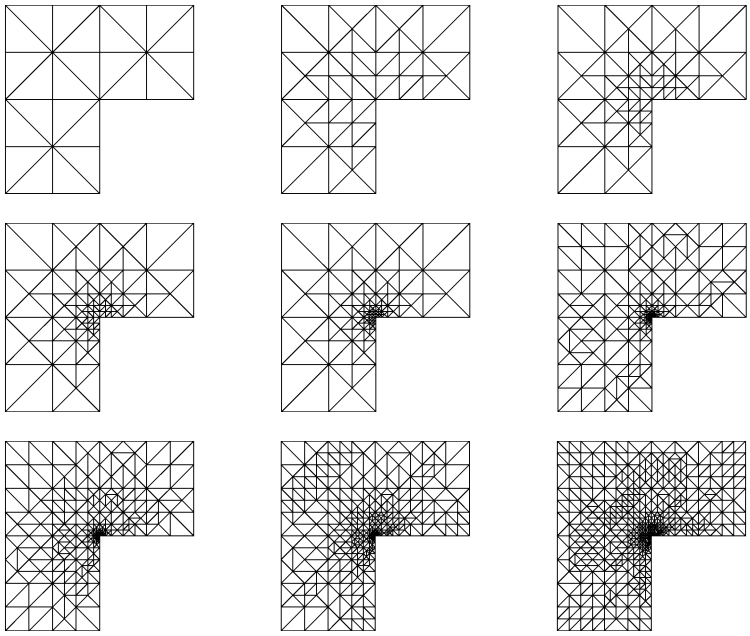

Figure 2: Sequence of adaptively refined meshes for Laplace example.

Ndofs	True	Estimated	Conforming	Non-conform	Effectivity
36	4.75(-1)	8.86(-1)	2.13(-1)	6.73(-1)	1.37
119	1.92(-1)	3.58(-1)	7.37(-2)	2.85(-1)	1.36
219	1.11(-1)	2.15(-1)	4.43(-2)	1.70(-1)	1.39
384	6.62(-2)	1.28(-1)	2.73(-2)	1.00(-1)	1.39
647	3.99(-2)	7.61(-2)	1.54(-2)	6.07(-2)	1.38
923	2.61(-2)	5.19(-2)	1.08(-2)	4.11(-2)	1.41
1377	1.84(-2)	3.62(-2)	7.94(-3)	2.82(-2)	1.40
2633	9.05(-3)	1.71(-2)	3.59(-3)	1.35(-2)	1.38
3302	7.10(-3)	1.36(-2)	3.06(-3)	1.05(-2)	1.38

Table 2: Comparison of estimated and true error for Poisson.

term chosen so that the solution is given by $u(r,\theta) = (r^{2/3} - r^2)\sin(2\theta/3)$. In this example, the conforming and non-conforming errors are both non-zero. The performance of the error estimator is shown in Table 2 along with the contributions from the conforming and non-conforming components of the error.

4.3 Variable permeability

The performance of the estimator in the case of variable permeability will be illustrated by considering the simple problem on the domain shown in Fig. 4 with scalar permeability $A = a_\ell I$ on Ω_ℓ and prescribed flux $g = \boldsymbol{n}\cdot\mathbf{grad}(x^2-y^2)$ on $\partial\Omega$. The true solution on subdomain Ω_ℓ is given by $u(x,y) = (x^2 - y^2)/a_\ell$. Consider the situation where the local permeability is given by $a_1 = 1$, $a_2 = \alpha^2$, $a_3 = 1$ and $a_4 = \alpha^4$ with an initial mesh consisting of four elements coinciding

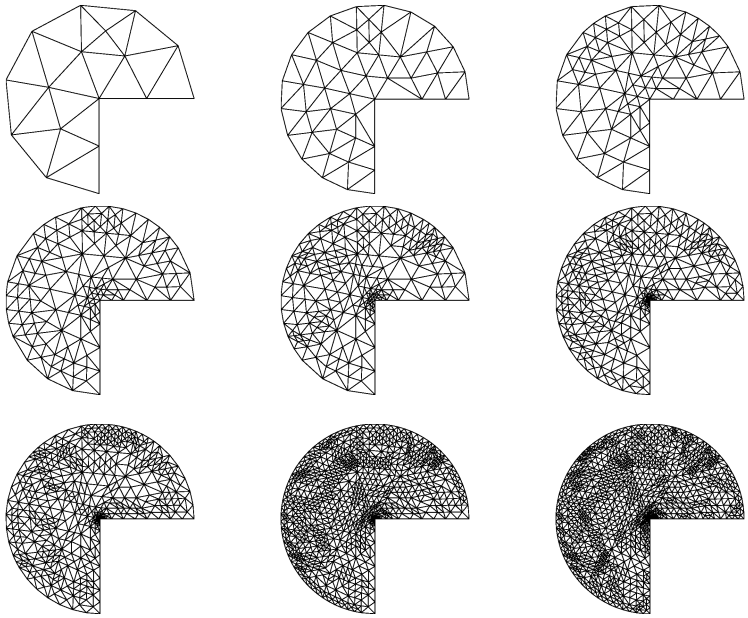

Figure 3: Sequence of adaptively refined meshes for Poisson problem.

with the sub-domains shown in Fig. (4).

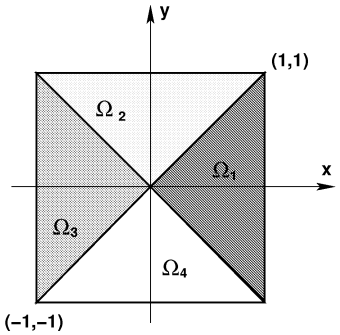

Figure 4: Geometry and subdomains for problem with variable permeability.

The ratio of the estimated error to the true error, $\mathrm{Eff}(\alpha)$, of the estimators obtained using the standard smoothing operator S with equal weighting and the estimator obtained using the weighted smoothing operator with weights depending on the permeability as in (18), can be computed explicitly on the initial mesh. For the standard scheme, we obtain

$$\mathrm{Eff}(\alpha)^2 = \begin{cases} \dfrac{3}{8}\alpha^4 + \mathcal{O}(1) & \text{as } \alpha \to \infty \\ \dfrac{15}{32}\alpha^{-4} + \mathcal{O}(\alpha^{-2}) & \text{as } \alpha \to 0 \end{cases}$$

whilst for the weighted estimator,

$$\mathrm{Eff}(\alpha)^2 = \begin{cases} \dfrac{27}{4} + \mathcal{O}(\alpha^{-1}) & \text{as } \alpha \to \infty \\ \dfrac{39}{8} + \mathcal{O}(\alpha) & \text{as } \alpha \to 0 \end{cases}$$

The performance of the standard estimator clearly degenerates rapidly as the local permeability α is varied. The performance of the estimators when α^2 is taken to be 0.1 is presented in in Fig. 5. As would be expected, as the mesh is refined, both estimators tend to give the same value. However, even with this relatively modest value of α, the standard scheme provides very poor estimates for the error on the coarser meshes. The distribution of the local error

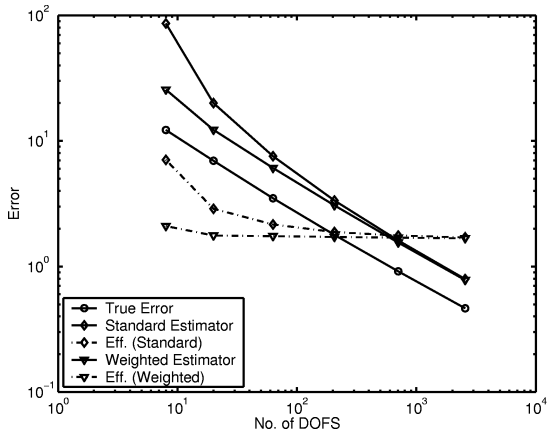

Figure 5: Comparison of standard estimator with weighted scheme for model problem with variable permeability.

estimates is compared with the actual local errors is shown in Fig. 6. Obviously, the estimators coincide away from interfaces. However, on interfaces and at the cross-point, it is observed that the weighted estimator gives a more accurate picture of the distribution of the true error. Here, the true error was used to construct the sequence of adaptively refined meshes. Essentially the same sequence of meshes would be obtained if the weighted estimator were used, whilst if the standard estimator were to be used, then one would obtain a completely different sequence of meshes.

4.4 Neither term can be dropped from the estimator

The fact that the estimator provides an upper bound for the solution of the Laplace equation shows that the non-conforming term must be present in the estimator. It is less clear that the interior residual term must also be present. Consider the Poisson equation on a unit square with pure Neumann data chosen so that the true solution is given by $3x^2 - 2xy + 3y^2$. Observe that the oscillation of f vanishes. Suppose that the solution is approximated using the

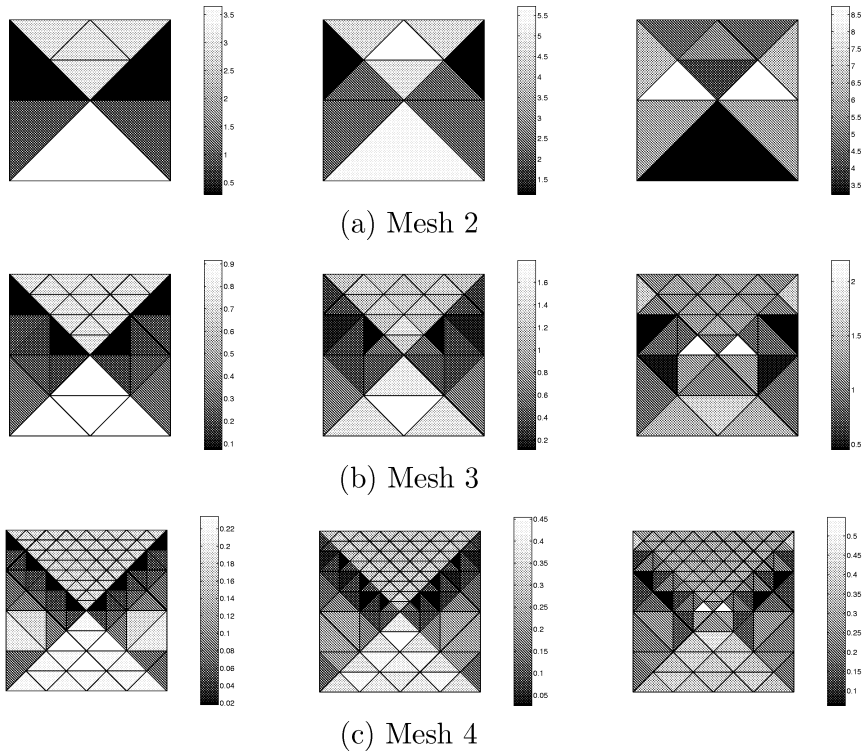

(a) Mesh 2

(b) Mesh 3

(c) Mesh 4

Figure 6: Distribution of true local error (left) and estimated local error for weighted (centre) and standard (right) estimators applied to model problem with variable permeability.

mesh obtained by sub-dividing the square into a uniform mesh of right-angled triangles with hypotenuse in the direction $(1, 1)$. In this scenario, it is found that the non-conforming finite element approximation u_{nc} is actually *conforming*, which means that the non-conforming term vanishes, yet the true error is obviously non-zero. This example shows that the interior residual term is essential for the upper bound, and therefore cannot be removed in general.

5 Estimation of the Conforming Error

5.1 Equilibrated Residual Method

The equilibrated residual method of a posteriori error estimation is based on the solution of independent local residual problems posed over each element K. The solution of the local problems is sought in the space

$$H_E^1(K) = \{v|_K : v \in H_E^1(\Omega)\} \tag{22}$$

consisting of restrictions of functions belonging to the space $H_E^1(\Omega)$ to a single element.

The equilibrated residual estimator requires a set of equilibrated fluxes. The functions $\{g_K \in L_2(\partial K) : K \in \mathcal{P}\}$ are said to be *equilibrated fluxes* if the

equilibration condition,

$$(f, v)_K + \int_{\partial K} g_K v \, \mathrm{d}s - (A \, \mathbf{grad}_{\mathsf{nc}} \, u_{\mathsf{nc}}, \mathbf{grad}_{\mathsf{nc}} \, v)_K = 0 \quad \forall v \in X^{\mathsf{nc}} \tag{23}$$

and the *consistency condition*

$$\sum_{K \in \mathcal{P}} \int_{\partial K} g_K v \, \mathrm{d}s = \int_{\Gamma_N} g v \, \mathrm{d}s \quad \forall v \in H^1_E(\Omega) \tag{24}$$

are satisfied. Given a set of equilibrated fluxes, the estimator is defined in terms of the solution $\varepsilon_K \in H^1_E(K)$ of the *local equilibrated residual problem*:

$$(A \, \mathbf{grad} \, \varepsilon_K, \mathbf{grad} \, v)_K = (f, v)_K + \int_{\partial K} g_K v \, \mathrm{d}s - (A \, \mathbf{grad}_{\mathsf{nc}} \, u_{\mathsf{nc}}, \mathbf{grad} \, v)_K, \tag{25}$$

for all $v \in H^1_E(K)$. The local error estimator is given by $(A \, \mathbf{grad} \, \varepsilon_K, \mathbf{grad} \, \varepsilon_K)_K$. The main property of this method is that it provides an upper bound on the error.

Lemma 2 *Let $\{g_K : K \in \mathcal{P}\}$ be a set of equilibrated fluxes. Then, there exist solutions $\{\varepsilon_K : K \in \mathcal{P}\}$ of the local residual problems (25). Moreover,*

$$(A \, \mathbf{grad} \, \phi, \mathbf{grad} \, \phi) \leq \sum_{K \in \mathcal{P}} (A \, \mathbf{grad} \, \varepsilon_K, \mathbf{grad} \, \varepsilon_K)_K. \tag{26}$$

The proof is practically identical to the argument used in the conforming case, see, for instance [2], and is therefore omitted.

Equilibrated fluxes are not uniquely determined by conditions (23)–(24). The construction of equilibrated fluxes for *conforming* finite elements is discussed in detail in [2]. One benefit of using the non-conforming elements is that it is markedly easier to define a set of equilibrated fluxes:

Lemma 3 *Let $g_K \in L_2(\partial K)$ be defined by the rule*

$$g_K = \frac{1}{h_\gamma} \{(\mathbf{grad}_{\mathsf{nc}} \, u_{\mathsf{nc}}, \mathbf{grad}_{\mathsf{nc}} \, \theta_\gamma)_K - (f, \theta_\gamma)_K\} \ \text{ on } \gamma \subset \partial K \backslash \Gamma_N \tag{27}$$

with $g_K = g$ on $\gamma \subset \partial K \cap \Gamma_N$. Then $\{g_K\}$ is a set of equilibrated fluxes.

Proof. It suffices to verify the equilibration condition (23) in the case $v = \theta_\gamma$. If $\gamma \not\subset \Gamma_N$, then

$$\int_{\partial K} g_K \theta_\gamma \, \mathrm{d}s = h_\gamma \, g_K|_\gamma = (\mathbf{grad}_{\mathsf{nc}} \, u_{\mathsf{nc}}, \mathbf{grad}_{\mathsf{nc}} \, \theta_\gamma)_K - (f, \theta_\gamma)_K$$

and the condition is satisfied. Alternatively, if $\gamma \subset \Gamma_N$ then θ_γ is supported on a single element K and the equilibration condition is equivalent to

$$(\mathbf{grad}_{\mathsf{nc}} \, u_{\mathsf{nc}}, \mathbf{grad} \, \theta_\gamma) = (f, \theta_\gamma) + \int_{\Gamma_N} g \theta_\gamma \, \mathrm{d}s$$

which is simply equation (4) with $v = \theta_\gamma$.

It remains to verify the consistency condition (24) holds. Suppose elements K and K' share the common edge γ. Then θ_γ is supported on $K \cup K'$ and so,

$$h_\gamma \, (g_K + g_{K'})|_\gamma = (f, \theta_\gamma) - (\mathbf{grad}_{\mathsf{nc}} \, u_{\mathsf{nc}}, \mathbf{grad}_{\mathsf{nc}} \, \theta_\gamma) = 0 \tag{28}$$

thanks to equation (4) with the choice $v = \theta_\gamma$. Let $v \in H^1_E(\Omega)$ then

$$\sum_{K \in \mathcal{P}} \int_{\partial K} g_K v \, \mathrm{d}s = \int_{\Gamma_N} g v \, \mathrm{d}s$$

since the contributions from the internal (shared) edges cancel pairwise in view of (28). □

We can take advantage of the explicit expression (27) for the equilibrated fluxes to simplify the data for the local residual problem (25). Let $v \in H^1_E(K)$ and let $\Pi_{\mathsf{nc}} \, v \in X^{\mathsf{nc}}$ denote the non-conforming interpolant. Applying integration by parts allows the right hand side of equation (25) to be rewritten as

$$(f, v)_K + \int_{\partial K} (g_K - \boldsymbol{n}_K \cdot A \, \mathbf{grad}_{\mathsf{nc}} \, u_{\mathsf{nc}}|_K) \, v \, \mathrm{d}s$$

since $\mathbf{div}(A \, \mathbf{grad}_{\mathsf{nc}} \, u_{\mathsf{nc}})$ vanishes. Now, thanks to the equilibration condition, the right hand side vanishes for $v \in X^{\mathsf{nc}}$ and we may replace v by $v - \Pi_{\mathsf{nc}} \, v$, giving the following expression for the right hand side of (25):

$$(f, v - \Pi_{\mathsf{nc}} \, v)_K + \int_{\partial K} (g_K - \boldsymbol{n}_K \cdot A \, \mathbf{grad}_{\mathsf{nc}} \, u_{\mathsf{nc}}|_K) \, (v - \Pi_{\mathsf{nc}} \, v) \, \mathrm{d}s.$$

Noting that $\int_\gamma \alpha (v - \Pi_{\mathsf{nc}} \, v) \, \mathrm{d}s$ vanishes for constants α, and that g_K and $A \, \mathbf{grad}_{\mathsf{nc}} \, u_{\mathsf{nc}}$ are constant on interior edges, the second term collapses to $\int_{\partial K \cap \Gamma_N} g(v - \Pi_{\mathsf{nc}} \, v) \, \mathrm{d}s$. In conclusion, we have the following alternative characterisation for the local equilibrated residual problem:

$$(A \, \mathbf{grad} \, \varepsilon_K, \mathbf{grad} \, v)_K = (f, v - \Pi_{\mathsf{nc}} \, v)_K + \int_{\partial K \cap \Gamma_N} g(v - \Pi_{\mathsf{nc}} \, v) \, \mathrm{d}s. \tag{29}$$

for all $v \in H^1_E(K)$. For future reference, we observe that equations (13) and (29) also yield an alternative expression for the conforming error defined in (13):

$$(A \, \mathbf{grad} \, \phi, \mathbf{grad} \, v) = (f, v - \Pi_{\mathsf{nc}} \, v) + \int_{\Gamma_N} g(v - \Pi_{\mathsf{nc}} \, v) \, \mathrm{d}s \tag{30}$$

for $v \in H^1_E(\Omega)$.

The upper bound of Lemma 2 holds regardless of the selection of equilibrated fluxes. However, the sharpness of bound depends on the particular choice. The next result shows that the construction given in Lemma 3 is quasi-optimal up to the addition of a higher order term measuring the local data oscillation.

Lemma 4 *Let $\{g_K\}$ be the equilibrated fluxes defined in Lemma 3. Then, there exists a constant C, independent of any mesh-size, such that*

$$\begin{aligned} &(A \, \mathbf{grad} \, \varepsilon_K, \mathbf{grad} \, \varepsilon_K)^{1/2}_K \\ &\quad \leq C \left\{ \Upsilon_K^{1/2} (A \, \mathbf{grad} \, \phi, \mathbf{grad} \, \phi)^{1/2}_K + \min(1, \lambda_K)^{-1/2} \Delta_K \right\} \end{aligned} \tag{31}$$

where $\Delta_K = \operatorname{osc}(f,K) + \operatorname{osc}(g,\{\gamma \subset \Gamma_N \cap \partial K\})$ *is the local data oscillation over element* K*.*

Proof. Let $v \in H^1_E(K)$. Then, since $\int_\gamma \overline{g}_\gamma(v - \Pi_{\mathsf{nc}}\, v)\,\mathrm{d}s$ vanishes for constant $\overline{g}_\gamma$, the right hand side of (29) may be rewritten as

$$(f, v - \Pi_{\mathsf{nc}}\, v)_K + \sum_{\gamma \subset \partial K \cap \Gamma_N} \int_\gamma (g - \overline{g}_\gamma)(v - \Pi_{\mathsf{nc}}\, v)\,\mathrm{d}s.$$

This may in turn be bounded above using (8),

$$C \left\{ h_K \left\| f \right\|_{L_2(K)} + \sum_{\gamma \subset \partial K \cap \Gamma_N} h_\gamma^{1/2} \left\| g - \overline{g}_\gamma \right\|_{L_2(\gamma)} \right\} \left\| \mathbf{grad}\, v \right\|_{L_2(K)},$$

Using the triangle inequality, the term in parentheses may be bounded above by

$$h_K \left\| \overline{f}_K \right\|_{L_2(K)} + \operatorname{osc}(f,K) + \sum_{\gamma \subset \partial K \cap \Gamma_N} h_\gamma^{1/2} \left\| g - \overline{g}_\gamma \right\|_{L_2(\gamma)}$$

while the multiplicative factor is bounded using (3),

$$\left\| \mathbf{grad}\, v \right\|_{L_2(K)} \leq \lambda_K^{-1/2} (A\, \mathbf{grad}\, v, \mathbf{grad}\, v)_K^{1/2}.$$

By choosing $v = \varepsilon_K$ in (29) and applying the Cauchy-Schwarz inequality, we find that

$$\begin{aligned} &(A\, \mathbf{grad}\, \varepsilon_K, \mathbf{grad}\, \varepsilon_K)_K^{1/2} \\ &\quad \leq C \lambda_K^{-1/2} \left\{ h_K \left\| \overline{f}_K \right\|_{L_2(K)} + \operatorname{osc}(f,K) + \operatorname{osc}(g,\{\gamma \subset \Gamma_N \cap \partial K\}) \right\}. \end{aligned} \tag{32}$$

Let $\chi \in H^1_0(K)$ be the cubic (bubble) function whose value is unity at the element centroid. Then, up to constants independent of the element size h_K,

$$\int_K \chi\,\mathrm{d}\boldsymbol{x} \approx h_K^2; \quad \left\| \chi \right\|_{L_2(K)} \approx h_K; \quad \left\| \mathbf{grad}\, \chi \right\|_{L_2(K)} \approx 1.$$

Thanks to (3), the latter estimate implies that $(A\, \mathbf{grad}\, \chi, \mathbf{grad}\, \chi)_K \leq C \Lambda_K$. Choosing $v = \chi$ in equation (30) gives

$$(A\, \mathbf{grad}\, \phi, \mathbf{grad}\, \chi) = (f, \chi)_K$$

since $\Pi_{\mathsf{nc}}\, \chi = 0$. Equally well, for constant $\overline{f}_K$,

$$\overline{f}_K (1, \chi)_K = (A\, \mathbf{grad}\, \phi, \mathbf{grad}\, \chi)_K - (f - \overline{f}_K, \chi)_K$$

and so, applying Cauchy-Schwarz inequalities and the properties of χ recorded above, we deduce that

$$\left| \overline{f}_K (1, \chi)_K \right| \leq C \left\{ \Lambda_K^{1/2} (A\, \mathbf{grad}\, \phi, \mathbf{grad}\, \phi)_K^{1/2} + h_K \left\| f - \overline{f}_K \right\|_{L_2(K)} \right\}.$$

Again exploiting properties of χ, we deduce that, up to constants independent of the mesh-size, $h_K \left\| \overline{f}_K \right\|_{L_2(K)} \approx \left| \overline{f}_K (1, \chi)_K \right|$ and hence

$$h_K \left\| \overline{f}_K \right\|_{L_2(K)} \leq C \left\{ \Lambda_K^{1/2} (A\, \mathbf{grad}\, \phi, \mathbf{grad}\, \phi)_K^{1/2} + \operatorname{osc}(f,K) \right\}. \tag{33}$$

Inserting this estimate into (32) gives the result as claimed. □

5.2 Inexact Solution of the Residual Problem

The solution of the local residual problem (25) cannot be computed exactly, and a practical alternative is required. Let $\overline{\boldsymbol{x}}_K$ denote the centroid of element K, and define

$$\boldsymbol{\sigma}_K = -\frac{1}{2}\overline{f}_K(\boldsymbol{x} - \overline{\boldsymbol{x}}_K) \tag{34}$$

where $\overline{f}_K$ denotes the (constant) average value of the data f on element K. The main result in this section is to show that the field σ_K may be used to define a computable estimator that provides reliable and efficient bounds on the true solution of the local residual problem (25) provided the data oscillation (9) is sufficiently small. Before turning to the main result, we first establish that the function σ_K has the following important property:

Lemma 5 *Let $\boldsymbol{\sigma}_K$ be defined as in (34). Then,*

$$(\boldsymbol{\sigma}_K, \mathbf{grad}\, v)_K = (\overline{f}_K, v - \Pi_{\mathsf{nc}}\, v)_K, \quad \forall v \in H^1_E(K). \tag{35}$$

Proof. Let $v \in H^1_E(K)$. Then, integration by parts gives

$$(\boldsymbol{\sigma}_K, \mathbf{grad}\, v)_K = -\int_K v\, \mathbf{div}\, \boldsymbol{\sigma}_K \,\mathrm{d}\boldsymbol{x} + \int_{\partial K} v\boldsymbol{n}_K \cdot \boldsymbol{\sigma}_K \,\mathrm{d}s$$

where $\boldsymbol{n}_K$ denotes the unit outward normal on ∂K. Inserting the expression for $\boldsymbol{\sigma}_K$ into the first term on the right hand side gives

$$-\int_K v\, \mathbf{div}\, \boldsymbol{\sigma}_K \,\mathrm{d}\boldsymbol{x} = (\overline{f}_K, v)_K$$

since $\overline{f}_K$ is constant. It therefore suffices to show that the second term satisfies

$$\int_{\partial K} v\boldsymbol{n}_K \cdot \boldsymbol{\sigma}_K \,\mathrm{d}s = -(\overline{f}_K, \Pi_{\mathsf{nc}}\, v)_K. \tag{36}$$

Substituting the expression for $\boldsymbol{\sigma}_K$ gives

$$\int_{\partial K} v\boldsymbol{n}_K \cdot \boldsymbol{\sigma}_K \,\mathrm{d}s = -\frac{1}{2}\overline{f}_K \sum_{\gamma \subset \partial K} \int_\gamma v\boldsymbol{n}_K \cdot (\boldsymbol{x} - \overline{\boldsymbol{x}}_K) \,\mathrm{d}s.$$

Elementary geometry reveals that $\boldsymbol{n}_K \cdot (\boldsymbol{x} - \overline{\boldsymbol{x}}_K)|_\gamma = 2\,\mathrm{meas}(K)/3\,\mathrm{meas}(\gamma)$, and hence

$$\int_\gamma v\boldsymbol{n}_K \cdot (\boldsymbol{x} - \overline{\boldsymbol{x}}_K) \,\mathrm{d}s = \frac{2}{3}\,\mathrm{meas}(K)\overline{v}_\gamma$$

where $\overline{v}_\gamma$ denotes the average value of v on the edge γ, and the left hand side of (36) may therefore be written in the form

$$\int_{\partial K} v\boldsymbol{n}_K \cdot \boldsymbol{\sigma}_K \,\mathrm{d}s = -\frac{1}{3}\,\mathrm{meas}(K)\overline{f}_K \sum_{\gamma \subset \partial K} \overline{v}_\gamma. \tag{37}$$

An elementary computation using (6) reveals that

$$\int_K \Pi_{\mathsf{nc}}\, v \,\mathrm{d}\boldsymbol{x} = \frac{1}{3}\,\mathrm{meas}(K) \sum_{\gamma \subset \partial K} \overline{v}_\gamma,$$

and the identity (36) now follows by combining this result with (37). □

The main result of this section may now be stated:

Theorem 6 *Let ε_K denote the solution of the approximate local residual problems (25) and $\boldsymbol{\sigma}_K$ denote the field given in (34). Then, there exist positive constants c and C, independent of any mesh-size, such that*

$$(A\,\mathbf{grad}\,\varepsilon_K, \mathbf{grad}\,\varepsilon_K)_K^{1/2} \leq \left(A^{-1}\boldsymbol{\sigma}_K, \boldsymbol{\sigma}_K\right)_K^{1/2} + C\lambda_K^{-1/2}\Delta_K \tag{38}$$

and

$$c(A^{-1}\boldsymbol{\sigma}_K, \boldsymbol{\sigma}_K)_K^{1/2} \leq \Upsilon_K^{1/2}(A\,\mathbf{grad}\,\phi, \mathbf{grad}\,\phi)_K^{1/2} + \lambda_K^{-1/2}\,\mathrm{osc}(f,K) \tag{39}$$

where Δ_K denotes the local data oscillation defined in Lemma 4.

Proof. Let $v \in H_E^1(K)$. Equations (29) and (35) imply that

$$\begin{aligned}&(A\,\mathbf{grad}\,\varepsilon_K - \boldsymbol{\sigma}_K, \mathbf{grad}\,v)_K \\ &\quad = (f - \overline{f}_K, v - \Pi_{\mathsf{nc}}\,v)_K + \int_{\partial K\cap\Gamma_N} g(v - \Pi_{\mathsf{nc}}\,v)\,\mathrm{d}s.\end{aligned} \tag{40}$$

The first term on the right hand side may be bounded using the Cauchy-Schwarz inequality and then applying (8) to obtain

$$(f - \overline{f}_K, v - \Pi_{\mathsf{nc}}\,v)_K \leq Ch_K \left\|f - \overline{f}_K\right\|_{L_2(K)} \|\mathbf{grad}\,v\|_{L_2(K)}\,.$$

Property (6) means that $\int_\gamma \overline{g}_\gamma(v - \Pi_{\mathsf{nc}}\,v)\,\mathrm{d}s$ vanishes for constant $\overline{g}_\gamma$, which enables us to rewrite the second term on the right hand side of (40) as

$$\sum_{\gamma\subset\partial K\cap\Gamma_N}\int_\gamma (g - \overline{g}_\gamma)(v - \Pi_{\mathsf{nc}}\,v)\,\mathrm{d}s.$$

Applying the Cauchy-Schwarz inequality and (8) reveals that

$$\int_{\partial K} g(v - \Pi_{\mathsf{nc}}\,v)\,\mathrm{d}s \leq C\,\|\mathbf{grad}\,v\|_{L_2(K)} \sum_{\gamma\subset\partial K\cap\Gamma_N} h_\gamma^{1/2}\left\|g - \overline{g}_\gamma\right\|_{L_2(\gamma)}.$$

With the aid of these estimates and (3), we obtain

$$\begin{aligned}(A\,\mathbf{grad}\,\varepsilon_K - \boldsymbol{\sigma}_K, \mathbf{grad}\,v)_K &\leq C\Delta_K\,\|\mathbf{grad}\,v\|_{L_2(K)} \\ &\leq C\lambda_K^{-1/2}\Delta_K(A\,\mathbf{grad}\,v, \mathbf{grad}\,v)_K^{1/2}.\end{aligned}$$

Now, choosing $v = \varepsilon_K$ we deduce that

$$\begin{aligned}&(A\,\mathbf{grad}\,\varepsilon_K, \mathbf{grad}\,\varepsilon_K)_K \\ &\quad\leq (\boldsymbol{\sigma}_K, \mathbf{grad}\,\varepsilon_K)_K + C\Delta_K\,\|\mathbf{grad}\,\varepsilon_K\|_{L_2(K)} \\ &\quad\leq \left\{(A^{-1}\boldsymbol{\sigma}_K, \boldsymbol{\sigma}_K)_K^{1/2} + C\lambda_K^{-1/2}\Delta_K\right\}(A\,\mathbf{grad}\,\varepsilon_K, \mathbf{grad}\,\varepsilon_K)_K^{1/2}\end{aligned}$$

which proves the upper bound. For the proof of the lower bound, we first use (3) and (16) to deduce that

$$(A^{-1}\boldsymbol{\sigma}_K, \boldsymbol{\sigma}_K)_K \leq C\lambda_K^{-1}h_K^2\left\|\overline{f}_K\right\|_{L_2(K)}^2.$$

and then, thanks to (33), we obtain

$$(A^{-1}\boldsymbol{\sigma}_K, \boldsymbol{\sigma}_K)_K^{1/2} \leq C\left\{\Upsilon_K^{1/2}(A\,\mathbf{grad}\,\phi, \mathbf{grad}\,\phi)_K^{1/2} + \lambda_K^{-1/2}\,\mathrm{osc}(f,K)\right\}$$

which completes the proof. □

6 Estimation of the Non-conforming Error

We turn to the problem of estimation of the non-conforming component of the total error defined by (14). The following result forms the basis for developing upper bounds.

Lemma 7 *Let ψ be defined in equation (14), then*

$$(A^{-1}\,\mathbf{curl}\;\psi, \mathbf{curl}\;\psi) = \min_{\substack{u^*\in H^1(\Omega):\\ u^*=q \text{ on } \Gamma_D}} (A\,\mathbf{grad}_{\mathsf{nc}}(u^*-u_{\mathsf{nc}}), \mathbf{grad}_{\mathsf{nc}}(u^*-u_{\mathsf{nc}})). \quad (41)$$

Proof. Let $u^* \in H^1(\Omega)$ satisfy $u^* = q$ on Γ_D. In particular, $u-u^* \in H^1_E(\Omega)$ and hence, applying Green's formula gives for each $w \in \mathcal{H}$,

$$(\mathbf{grad}_{\mathsf{nc}}(u-u^*), \mathbf{curl}\, w) = \int_{\partial\Omega} (u-u^*)\frac{\partial w}{\partial s}\,\mathrm{d}s = 0$$

since the first term vanishes on Γ_D while the second vanishes on Γ_N. Consequently,

$$(A^{-1}\,\mathbf{curl}\;\psi, \mathbf{curl}\, w) = (\mathbf{grad}_{\mathsf{nc}}\, e, \mathbf{curl}\, w) = (\mathbf{grad}_{\mathsf{nc}}(u^*-u_{\mathsf{nc}}), \mathbf{curl}\, w).$$

Therefore, choosing $w = \psi$ and applying a Cauchy-Schwarz inequality reveals that

$$(A^{-1}\,\mathbf{curl}\;\psi, \mathbf{curl}\;\psi) \le (A\,\mathbf{grad}_{\mathsf{nc}}(u^*-u_{\mathsf{nc}}), \mathbf{grad}_{\mathsf{nc}}(u^*-u_{\mathsf{nc}})).$$

It remains to show the lower bound is attained. Let $\phi \in H^1_E(\Omega)$ be defined as in equation (13), and choose u^* to be the function $u-\phi$. Identity (12) reveals that

$$A\,\mathbf{grad}_{\mathsf{nc}}(u^*-u_{\mathsf{nc}}) = A\,\mathbf{grad}_{\mathsf{nc}}(e-\phi) = \mathbf{curl}\;\psi$$

which shows the lower bound is attained. □

The significance of Lemma 7 is, given *any* admissible function u^* in equation (41), we immediately obtain an upper bound on the non-conforming error. The accuracy of the bound will of course depend on the particular choice of function u^*. Equally well, the ease with which the bound may be evaluated will depend on the actual form of the function. Simple choices of u^* are ruled out by the condition on the Dirichlet boundary (except those where the Dirichlet data q is trivial), and it will be worthwhile to relax this restriction (at the expense of introducing an oscillation term for the Dirichlet data). We shall base our choice of u^* on a continuous, piecewise affine function $\mathcal{S}(u_{\mathsf{nc}})$ obtained by post-processing the non-conforming approximation. The restriction of the function $\mathcal{S}(u_{\mathsf{nc}})$ to the Dirichlet boundary is chosen to be the continuous piecewise linear interpolant q_I of the Dirichlet data q at element vertices on Γ_D.

Lemma 8 *Let $\mathcal{S}(u_{\mathsf{nc}})$ be any piecewise affine function whose restriction to the Dirichlet boundary Γ_D coincides with q_I. Then, there exists a constant C independent of any mesh-size, such that*

$$\begin{aligned}(A^{-1}\,\mathbf{curl}\;\psi, \mathbf{curl}\;\psi)^{1/2} \;&\le\; (A\,\mathbf{grad}_{\mathsf{nc}}(u_{\mathsf{nc}}-\mathcal{S}(u_{\mathsf{nc}})), \mathbf{grad}_{\mathsf{nc}}(u_{\mathsf{nc}}-\mathcal{S}(u_{\mathsf{nc}})))^{1/2} \\ &+\; C\Lambda_{\Gamma_D}^{1/2}\,\mathrm{osc}\,(\partial q/\partial s, \{\gamma : \gamma \subset \Gamma_D\}) \qquad (42)\end{aligned}$$

where $\Lambda_{\Gamma_D} = \max\{\Lambda_K : K \text{ has an edge on } \Gamma_D\}$.

Proof. First, let $\gamma \subset \partial\mathcal{P} \cap \Gamma_D$ and observe that $q - q_I \in H^{1/2}_{00}(\gamma)$. Moreover, the convexity of the $H^{1/2}_{00}$-norm and standard (one-dimensional) approximation properties of the interpolant reveal that

$$\|q - q_I\|^2_{H^{1/2}_{00}(\gamma)} \leq C h_\gamma \, \|\partial q/\partial s\|^2_{L_2(\gamma)} \, .$$

The same argument applies if we replace q by $q - \alpha s$, where $\alpha \in \mathbb{R}$ is arbitrary and s denotes the arc-length, yielding the estimate

$$\|q - q_I\|_{H^{1/2}_{00}(\gamma)} \leq C \, \mathrm{meas}(\gamma) \inf_{\alpha \in \mathbb{R}} \|\partial q/\partial s - \alpha\|^2_{L_2(\gamma)} = C \, \mathrm{osc}(\partial q/\partial s, \gamma)^2. \quad (43)$$

The function u^* is then chosen to be $u^* = \mathcal{S}(u_{\mathsf{nc}}) + \xi$. The function $\xi \in H^1(\Omega)$ is defined element-wise by $\xi_{|K} = q - q_I$ on $\partial K \cap \Gamma_D$, $\xi_{|K} = 0$ on $\partial K \backslash \Gamma_D$ and extended onto the domain interior as a harmonic function so that $\|\xi\|_{H^1(K)} \leq C \, \|q - q_I\|_{H^{1/2}_{00}(\partial K \cap \Gamma_D)}$. Hence, thanks to (3) and (43),

$$(A \, \mathbf{grad}\, \xi, \mathbf{grad}\, \xi)^{1/2} \leq C \Lambda_K^{1/2} \, \mathrm{osc}(\partial q/\partial s, \{\gamma : \gamma \subset \Gamma_D\}).$$

Inserting this choice of u^* in Lemma 7 and applying the triangle inequality gives the result claimed. □

6.1 Local Smoothing Operator

Given a particular choice of the function $S(u_{\mathsf{nc}})$, Lemma 8 shows how to obtain computable upper The tightness of the bound and the efficiency of the resulting estimator will hinge on the particular construction chosen for S.

The affine function $\mathcal{S}(u_{\mathsf{nc}})$ is uniquely defined by the values at the nodes of the partition given in equation (17). It is clear that S is a linear operator. The next result shows that S is continuous and can be bounded in terms of the choice of weights and the path permeability between elements discussed in Sect. 2.4:

Lemma 9 *Let $n \in \mathcal{N}$ and $K \in \Omega_n$. Then*

$$\begin{aligned} &\left|u_{\mathsf{nc}|K}(\boldsymbol{x}_n) - \mathcal{S}(u_{\mathsf{nc}})(\boldsymbol{x}_n)\right| \\ &\qquad \leq C \begin{cases} \left(A^{-1} \, \mathbf{curl}\, \psi, \mathbf{curl}\, \psi\right)^{1/2}_{\Omega_n} \sum_{K' \subset \Omega_n} \omega_{K',n} \lambda^{-1/2}_{KK'}, & \text{if } \boldsymbol{x}_n \notin \Gamma_D \\ \lambda^{-1/2}_{K\Gamma_D} \left(A^{-1} \, \mathbf{curl}\, \psi, \mathbf{curl}\, \psi\right)^{1/2}_{\Omega_n} + \mathrm{osc}(\partial q/\partial s, \{\gamma \in \mathcal{E}_n \cap \Gamma_D\}), & \\ \qquad\qquad \text{if } \boldsymbol{x}_n \in \Gamma_D. \end{cases} \end{aligned}$$

Proof. Case (i): $\boldsymbol{x}_n \notin \Gamma_D$. Inserting definition (17) and using property (19), we obtain

$$u_{\mathsf{nc}|K}(\boldsymbol{x}_n) - \mathcal{S}(u_{\mathsf{nc}})(\boldsymbol{x}_n) = \sum_{K' \subset \Omega_n} \omega_{K',n} \left(u_{\mathsf{nc}|K}(\boldsymbol{x}_n) - u_{\mathsf{nc}|K'}(\boldsymbol{x}_n)\right). \quad (44)$$

To begin with, we consider the contribution to this quantity arising when an element K' shares a common edge γ with element K. An elementary computation reveals that

$$u_{\mathsf{nc}|K}(\boldsymbol{x}_n) - u_{\mathsf{nc}|K'}(\boldsymbol{x}_n) = \frac{h_\gamma}{2} \left[\frac{\partial \, u_{\mathsf{nc}}}{\partial s}\right]_\gamma, \quad \gamma = \partial K \cap \partial K'. \quad (45)$$

Let β_γ denote the continuous piecewise quadratic function that takes the value 3/4 at the midpoint of edge γ and vanishes at all remaining nodes and midpoints. The function β_γ is supported on the patch $K \cup K'$. In equation (14), we choose $w \in \mathcal{H}$ to be the difference between β_γ and its (constant) average value over the domain Ω to obtain

$$(A^{-1}\,\mathbf{curl}\;\psi, \mathbf{curl}\;\beta_\gamma)_{K\cup K'} = (\mathbf{grad}_{\mathsf{nc}}\, e, \mathbf{curl}\;\beta_\gamma).$$

Integration by parts allows the right hand side to be rewritten in the form

$$(A^{-1}\,\mathbf{curl}\;\psi, \mathbf{curl}\;\beta_\gamma)_{K\cup K'} = \int_\gamma \left[\frac{\partial\, u_{\mathsf{nc}}}{\partial s}\right]_\gamma \beta_\gamma \,\mathrm{d}s = \frac{h_\gamma}{2}\left[\frac{\partial\, u_{\mathsf{nc}}}{\partial s}\right]_\gamma$$

where the fact that the jump is constant on an interior edge has been used. Together with (45), this identity implies

$$u_{\mathsf{nc}|K}(\boldsymbol{x}_n) - u_{\mathsf{nc}|K'}(\boldsymbol{x}_n) = (A^{-1}\,\mathbf{curl}\;\psi, \mathbf{curl}\;\beta_\gamma)_{K\cup K'}. \tag{46}$$

This relation is valid for pairs of elements K and K' sharing a common edge γ. More generally, suppose elements K and K' share only a common node $\boldsymbol{x}_n$. The path $\wp^*(K, K')$ appearing in (10) links the elements through a set of edges having an endpoint at $\boldsymbol{x}_n$. Relation (46) holds on each edge along the path, and so, by summing (46) over edges, we obtain a telescoping sum of differences of u_{nc} across neighbouring edges which simplifies to give

$$u_{\mathsf{nc}|K}(\boldsymbol{x}_n) - u_{\mathsf{nc}|K'}(\boldsymbol{x}_n) = \left(A^{-1}\,\mathbf{curl}\;\psi, \mathbf{curl}\;\beta_{KK'}\right)$$

where $\beta_{KK'} = \sum_{\gamma\in\wp^*(K,K')} \beta_\gamma$. Here, with a harmless overloading of notation, $\wp^*(K, K')$ is used to denote edges on the path. Applying the Cauchy-Schwarz inequality gives the upper bound

$$\begin{aligned}&\left|u_{\mathsf{nc}|K}(\boldsymbol{x}_n) - u_{\mathsf{nc}|K'}(\boldsymbol{x}_n)\right| \\ &\quad\le \left(A^{-1}\,\mathbf{curl}\;\psi, \mathbf{curl}\;\psi\right)_{\Omega_n}^{1/2} \left(A^{-1}\,\mathbf{curl}\;\beta_{KK'}, \mathbf{curl}\;\beta_{KK'}\right)^{1/2}.\end{aligned} \tag{47}$$

The permeability on each element in the path $\wp^*(K, K')$ is bounded below by $\lambda_{KK'}$ implying that

$$\left(A^{-1}\,\mathbf{curl}\;\beta_{KK'}, \mathbf{curl}\;\beta_{KK'}\right) \le \lambda_{KK'}^{-1}\,\|\mathbf{curl}\;\beta_{KK'}\|^2 \le C\lambda_{KK'}^{-1}$$

where C is independent of any mesh-size. Inserting this estimate into (47) and recalling (44) completes the proof in the first case.

Case (ii): If $\boldsymbol{x}_n \in \Gamma_D$, then $\mathcal{S}(u_{\mathsf{nc}})$ interpolates the Dirichlet data q at the node, so

$$u_{\mathsf{nc}|K}(\boldsymbol{x}_n) - \mathcal{S}(u_{\mathsf{nc}})(\boldsymbol{x}_n) = u_{\mathsf{nc}|K}(\boldsymbol{x}_n) - q(\boldsymbol{x}_n).$$

First consider the case when element K abuts the Dirichlet boundary Γ_D. It is not difficult to show that

$$u_{\mathsf{nc}|K}(\boldsymbol{x}_n) - q(\boldsymbol{x}_n) = \frac{h_\gamma}{2}\left.\frac{\partial\, u_{\mathsf{nc}}}{\partial s}\right|_\gamma - \left(q(\boldsymbol{x}_n) - q(\boldsymbol{m}_\gamma)\right). \tag{48}$$

Let μ_γ denote the average value of $\partial q/\partial s$ on edge γ, then, again using (14), we obtain

$$\left(A^{-1}\,\mathbf{curl}\;\psi,\mathbf{curl}\;\beta_\gamma\right)=\frac{h_\gamma}{2}\left.\frac{\partial\,u_{\mathsf{nc}}}{\partial s}\right|_\gamma-\int_\gamma\left(\frac{\partial q}{\partial s}-\mu_\gamma\right)\beta_\gamma\,\mathrm{d}s-\frac{1}{2}\left(q(\boldsymbol{x}_n)-q(\boldsymbol{x}_m)\right).$$

Subtracting this from (48) gives

$$\begin{aligned}&u_{\mathsf{nc}|K}(\boldsymbol{x}_n)-\mathcal{S}(u_{\mathsf{nc}})(\boldsymbol{x}_n)\\&\quad=\left(A^{-1}\,\mathbf{curl}\;\psi,\mathbf{curl}\;\beta_\gamma\right)+\int_\gamma\left(\frac{\partial q}{\partial s}-\mu_\gamma\right)\beta_\gamma\,\mathrm{d}s+q(\boldsymbol{m}_\gamma)-\frac{1}{2}\left(q(\boldsymbol{x}_n)+q(\boldsymbol{x}_m)\right).\end{aligned}$$

Applying the Peano Kernel Theorem [11], we write

$$q(\boldsymbol{m}_\gamma)-\frac{1}{2}\left(q(\boldsymbol{x}_n)+q(\boldsymbol{x}_m)\right)=\int_\gamma\frac{\partial q}{\partial s}w\,\mathrm{d}s=\int_\gamma\left(\frac{\partial q}{\partial s}-\mu_\gamma\right)w\,\mathrm{d}s$$

where $w=1/2$ on $(\boldsymbol{x}_m,\boldsymbol{m}_\gamma)$ and $w=-1/2$ on $(\boldsymbol{m}_\gamma,\boldsymbol{x}_n)$. As a consequence, we obtain

$$u_{\mathsf{nc}|K}(\boldsymbol{x}_n)-\mathcal{S}(u_{\mathsf{nc}})(\boldsymbol{x}_n)=\left(A^{-1}\,\mathbf{curl}\;\psi,\mathbf{curl}\;\beta_\gamma\right)+\int_\gamma\left(\frac{\partial q}{\partial s}-\mu_\gamma\right)(\beta_\gamma-w)\;\mathrm{d}s.$$

Bounding the second term above by the oscillation of $\partial q/\partial s$ on γ, leads to the estimate

$$\begin{aligned}&\left|u_{\mathsf{nc}|K}(\boldsymbol{x}_n)-\mathcal{S}(u_{\mathsf{nc}})(\boldsymbol{x}_n)\right|\\&\qquad\le C\lambda_{K\Gamma_D}^{-1/2}\left(A^{-1}\,\mathbf{curl}\;\psi,\mathbf{curl}\;\psi\right)_{\Omega_n}^{1/2}+C\,\mathrm{osc}(\partial q/\partial s,\gamma).\end{aligned}$$

This proves the result in the case of an element $K\in\Omega_n$ which has an edge γ on Γ_D. The result may be extended to cover a general element $K'\subset\Omega_n$ by connecting to the exterior boundary along the path $\wp^*(K,\Gamma_D)$, and arguing as before. □

6.2 Efficiency of the Estimator

The next result concerns the efficiency of the estimator when the weights are chosen as in (18).

Theorem 10 *Let $\mathcal{S}(u_{\mathsf{nc}})$ denote the post-processed approximation defined in equation (17). If $K\in\mathcal{P}$ has no vertices belonging to Γ_D, then there exists a positive constant c, independent of any mesh-size, such that*

$$\begin{aligned}&c\left(A\,\mathbf{grad}_{\mathsf{nc}}(u_{\mathsf{nc}}-\mathcal{S}(u_{\mathsf{nc}})),\mathbf{grad}_{\mathsf{nc}}(u_{\mathsf{nc}}-\mathcal{S}(u_{\mathsf{nc}}))\right)_K\\&\qquad\le\left(A^{-1}\,\mathbf{curl}\;\psi,\mathbf{curl}\;\psi\right)_{\widetilde{K}}\sum_{K'\subset\widetilde{K}}\Upsilon_{KK'}\end{aligned}\tag{49}$$

where $\widetilde{K}$ denotes the patch formed from those elements sharing a common vertex with element K. In the case where K has a vertex $\boldsymbol{x}_n\in\Gamma_D$, then the same estimate holds if the right hand side is supplemented with the term

$$\Upsilon_{K\Gamma_D}\left(A^{-1}\,\mathbf{curl}\;\psi,\mathbf{curl}\;\psi\right)_{\widetilde{K}}+\mathrm{osc}(\partial q/\partial s,\{\gamma\in\mathcal{E}_n\cap\Gamma_D\})^2.\tag{50}$$

Proof. Applying (3) and an inverse estimate shows the left hand side of (49) is bounded above by

$$C\Lambda_K h_K^{-2} \left\| u_{\mathsf{nc}} - \mathcal{S}(u_{\mathsf{nc}}) \right\|_{L_2(K)}^2$$

and then evaluating this integral (using, for instance, the quadrature rule based on edge midpoints which is exact for quadratic functions) gives

$$C\Lambda_K \sum_{\gamma \subset \partial K} \left| u_{\mathsf{nc}}(\boldsymbol{m}_\gamma) - \mathcal{S}(u_{\mathsf{nc}})(\boldsymbol{m}_\gamma) \right|^2 .$$

The restriction of $u_{\mathsf{nc}|K} - \mathcal{S}(u_{\mathsf{nc}})$ to an edge $\gamma \subset \partial K$ is a linear function of arc-length, which means that the value at the midpoint $\boldsymbol{m}_\gamma$ is the average of the values at the endpoints of the edge, and therefore,

$$\left| u_{\mathsf{nc}}(\boldsymbol{m}_\gamma) - \mathcal{S}(u_{\mathsf{nc}})(\boldsymbol{m}_\gamma) \right| \leq \frac{1}{2} \sum_{\boldsymbol{x}_n \in \gamma} \left| u_{\mathsf{nc}|K}(\boldsymbol{x}_n) - \mathcal{S}(u_{\mathsf{nc}})(\boldsymbol{x}_n) \right| .$$

Hence,

$$\begin{aligned} &\left(A \, \mathbf{grad}_{\mathsf{nc}}(u_{\mathsf{nc}} - \mathcal{S}(u_{\mathsf{nc}})), \mathbf{grad}_{\mathsf{nc}}(u_{\mathsf{nc}} - \mathcal{S}(u_{\mathsf{nc}})) \right)_K \\ &\qquad \leq C\Lambda_K \sum_{\boldsymbol{x}_n \in K} \left| u_{\mathsf{nc}|K}(\boldsymbol{x}_n) - \mathcal{S}(u_{\mathsf{nc}})(\boldsymbol{x}_n) \right|^2 . \end{aligned} \tag{51}$$

Suppose that no vertex of K belongs to Γ_D, then the first estimate in Lemma 9 gives the following upper bound for (51)

$$\sum_{\boldsymbol{x}_n \in K} \left(A^{-1} \, \mathbf{curl} \, \psi, \mathbf{curl} \, \psi \right)_{\Omega_n} \sum_{K' \subset \Omega_n} \frac{\min(\Lambda_K, \Lambda_{K'})}{\lambda_{KK'}}$$

which in turn may be bounded above by the right hand side of (51). If K has a vertex $\boldsymbol{x}_n \in \Gamma_D$, then the second estimate in Lemma 9 must be used, which gives rise to the additional term (50). □

References

[1] A. Agouzal. A posteriori error estimator for nonconforming finite element methods. *Appl. Math. Lett.*, 7(5):1017–1033, September 1994.

[2] M. Ainsworth and J.T. Oden. *A Posteriori Error Estimation in Finite Element Analysis.* John Wiley & Sons, 2000.

[3] W.Z. Bao and J.W. Barrett. A priori and a posteriori error bounds for a nonconforming linear finite element approximation of a non-Newtonian flow. *RAIRO Modél. Math. Anal. Numér.*, 32(7):843–858, December 1998.

[4] C. Bernardi and R. Verfürth. Adaptive finite element methods for elliptic equations with non-smooth coefficients. *Numer. Math.*, 85:579–608, 2000.

[5] S.C. Brenner and L.R. Scott. *The Mathematical Theory of Finite Element Methods*, volume 15 of *Texts in Applied Mathematics*. Springer-Verlag, New York, 1994.

[6] C. Carstensen, S. Bartels, and S. Jansche. A posteriori error estimates for nonconforming finite element methods. *Numer. Math.*, 92(2):233–256, 2002.

[7] P. G. Ciarlet. *The Finite Element Method for Elliptic Problems*. Elsevier, North-Holland, 1978.

[8] M. Crouzeix and P.A. Raviart. Conforming and nonconforming finite element methods for solving the stationary Stokes equations. *RAIRO Modél. Math. Anal. Numér.*, 3:33–75, 1973.

[9] E. Dari, R. Duran, and C. Padra. Error estimators for nonconforming finite-element approximations of the Stokes problem. *Math. Comp.*, 64(211):1017–1033, July 1995.

[10] E. Dari, R. Duran, C. Padra, and V. Vampa. A posteriori error estimators for nonconforming finite element methods. *RAIRO Modél. Math. Anal. Numér.*, 30(4):385–400, 1996.

[11] P.J. Davis. *Interpolation and Approximation*. Dover, 1976.

[12] P. Destuynder and B. Metivet. Explicit error bounds for a nonconforming finite element method. *SIAM J. Numer. Anal.*, 35(5):2099–2115, October 1998.

[13] W. Dörfler and R. H. Nochetto. Small data oscillation implies the saturation assumption. *Numer. Math.*, 91(1):1–12, 2002.

[14] V. Girault and P.A. Raviart. *Finite Element Methods for Navier Stokes Equations*, volume 5 of *Springer Series in Computational Mathematics*. Springer-Verlag, 1986.

[15] R.H.W. Hoppe and B. Wohlmuth. Element-oriented and edge-oriented local error estimators for nonconforming finite element methods. *RAIRO Modél. Math. Anal. Numér.*, 30:237–263, 1996.

[16] P. Oswald. Intergrid transfer operators and multilevel preconditioners for nonconforming discretizations. *Appl. Numer. Math.*, 23(1):139–158, February 1997.

[17] F. Schieweck. A posteriori error estimates with post-processing for nonconforming finite elements. *ESAIM Math. Mod. Numer. Anal.*, 36(3):489–503, May/June 2002.